Journal of Magnetic Resonance **156,** 309–312 (2002)
doi:10.1006/jmre.2002.2547

COMMUNICATIONS

A Double End-Cap Birdcage RF Coil for Small Animal Whole Body Imaging

Gultekin Gulsen, L. Tugan Muftuler, and Orhan Nalcioglu

John Tu and Thomas Yuen Center for Functional Onco-Imaging, University of California, Irvine, California

Received June 4, 2001; revised April 9, 2002; published online July 3, 2002

Proper design of a birdcage coil plays a very important role in obtaining high-resolution small animal magnetic resonance imaging. The RF field homogeneity and the coil filling factor directly affect the signal-to-noise ratio (S/N) and therefore limit the resolution. It has been shown that a conductive end-cap placed on one side of the coil can improve the RF field inhomogeneity near this area. This also contributes to an increase in the S/N by reducing the length of the RF coil. While this is true near the end-cap, the distal half of the coil still suffers from poor homogeneity and S/N. Consequently, such a shortfall may hinder small animal whole body imaging. In order to improve the coil performance for a larger imaging volume, we designed a new small animal birdcage RF coil by adding a detachable second end-cap to the open end. The performance of single end and double end RF coils was compared experimentally. The results indicate that the double end-cap can provide superior uniformity along the long axis of the coil. Furthermore, if one wishes to obtain the same homogeneity within a given volume, a double end-cap would have less than half of the length of the single end-cap coil leading to a superior S/N performance.

Key Words: **MRI; birdcage; end-cap; instrumentation; RF coil.**

INTRODUCTION

A conductive end-cap is generally used to improve the RF field homogeneity and signal-to-noise ratio (S/N), and lower coil losses in low-pass birdcage coils (*1*). The end-cap serves as a mirror and provides the desired homogeneity in the volume of a birdcage coil near the end-cap (*2, 3*). This makes it possible to use shorter coils with an end-cap to obtain the desired homogeneity. At high frequencies the length of the conductive legs becomes comparable with the wavelength of the RF field. Therefore shorter legs and a higher filling factor can be obtained by using an end-cap. However, the RF field strength falls off near the open end due to finite length of the cylinder. The high concentration of current in the end ring also affects the homogeneity around this end. Due to these reasons, field inhomogeneity is observed only within the volume of the birdcage coil near the open end. This is especially important for whole body imaging such as dynamic contrast enhancement studies in which the image slices are prescribed through both tumor and liver regions (*4*). The purpose of the current study was to investigate the addition of a detachable end-cap to this open end and therefore to provide improved RF field homogeneity throughout the entire volume enclosed by the birdcage coil. The coil performance was assessed using the S/N as a function of position along the long axis of the RF coil.

METHOD

We constructed a single end-cap RF coil in order to compare its performance against a double end-cap coil with identical physical dimensions. The coil was 12.6 cm in diameter and 15 cm in length. It was a low-pass transmit–receive design and consisted of eight legs. It was driven through capacitive coupling to two quadrature modes (*5*). The end-cap had eight radial slits. Each slit was bridged by two 1000-pF capacitors. The radial locations of the capacitors were 2.1 and 4.2 cm. The second end-cap with the same capacitor values and locations was used to replace the end-ring at the open end after the images were taken with the first end-cap. Gold plated pin and socket contacts were used for the second end-cap to provide detachability (Fig. 1). The study was performed using a 3-T scanner with a head gradient coil. A phantom filled with $CuSo_4$ solution was used to test each coil. The phantom had a diameter of 7.6 cm and was 13 cm in length. Images were acquired using a 2D spin–echo pulse sequence with 5-mm thickness, 16-cm FOV, and TR/TE = 800/15 ms. Flip angle was 90° and the acquisition matrix size was 128×256. In order to determine the reproducibility, the images of the phantom were acquired 10 times with the double end-cap coil and in each case the end-cap was detached and attached again. Whenever the end-cap was replaced, its orientation was always kept the same with the aid of visual markers placed on both the coil and the end-cap itself.

RESULTS

The axial images obtained using both coils were analyzed for quantifying respective performance. The phantom was placed in

1090-7807/02 $35.00

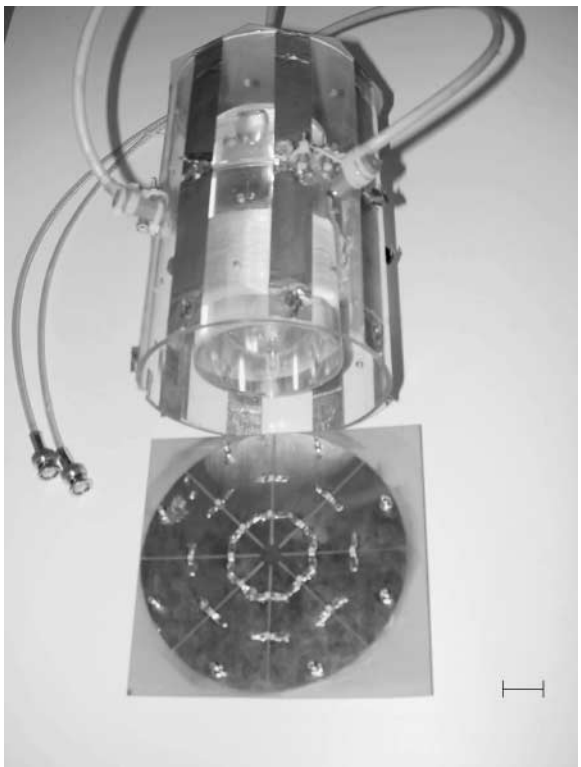

FIG. 1. The double end-cap coil. The second end-cap is detachable. Gold-plated socket and pin contacts were used. The horizontal bar shown in the figure corresponds to a distance of 2 cm.

the center of each RF coil with the RF coil being aligned in the center of the gradient coil. The slice thickness was 5 mm and 13 slices with an interslice gap of 5 mm were acquired to cover the entire phantom. The reason we included a 5-mm slice gap was to avoid any interslice contribution in our measurements. Since we used a 30-cm diameter head-insert gradient coil, the linear region of the gradient fields was smaller compared to the length of the phantom. Therefore, both ends of the phantom experience lower gradient fields which results in larger FOV for the several slices located at both ends. This in turn causes deceptively higher S/N in the end slices if a circular ROI smaller than the size of the phantom image is selected to calculate the mean signal. We observed that the FOV increased as much as 20% for the last slices at both ends. Since the size of the coil was designed for whole-body rat imaging we could not reduce the length of the coil. To eliminate the gradient nonlinearity effect, first the edge of the image and the corresponding area was determined for each slice. Afterward, a circular ROI corresponding to this area was selected for each slice. The mean signal was multiplied by the area and normalized with respect to the area of the center slice ($z = 0$) according to

$$\langle Signal_{norm}(i)\rangle = \langle Signal(i)\rangle * \frac{Area(i)}{Area(z=0)}, \qquad [1]$$

where $\langle\cdot\rangle$ is the average value of the quantity in the brackets and i is the slice number with $i = 1, \ldots, 13$. In Eq. [1] $Area(i)$ means the area of the circular phantom in slice i and $z = 0$ corresponds to $i = 7$. The standard deviation of the background noise was found by selecting four squares from the four corners of the image and taking the mean of the standard deviation of all individual squares. The signal-to-noise ratio for each slice was calculated by taking the ratio of the normalized mean signal to the mean standard deviation of the background noise.

$$S/N(i) = \langle Signal_{norm}(i)\rangle / \langle noise(i)\rangle \qquad [2]$$

The error in the signal-to-noise ratio was found by calculating the standard deviation of the signal-to-noise ratio for 10 consecutive acquisitions which was 0.5 and 1.8% for the single and double end-cap coils, respectively. The signal-to-noise ratios as defined in Eq. [2] for the single and double end-cap coils are shown in Fig. 2. It is seen that the single end-cap has a good S/N performance near the closed end; however, its performance decreases drastically near the open end as expected. Figure 2 shows that the double end-cap coil has an excellent SNR along the z-axis from one end to the other. The difference in the signal-to-noise ratio for the two coils for one half of the coil volume toward the fixed end-cap is negligible. However, the signal-to-noise ratio of the double end-cap coil increases by approximately 11% at the removable end-cap side with respect to the center while it decreases approximately by 30% in the same region for the single end-cap coil. This shows that the double end-cap birdcage coil has a superior S/N performance throughout its length, especially when compared to the single end-cap in the region of the open end-cap for the later coil. The measurement of the in-plane homogeneity was performed by comparing the homogeneity of both coils along the x- and y-axes for each slice. Figure 3 shows the signal profiles along the x- and y-axes for slices 1, 7, and 13. The locations of these slices are defined in Fig. 2. The maximum change in the x-profile was around 2% and the maximum change in the y-profile was around 6% between slices 7 and 13 for both

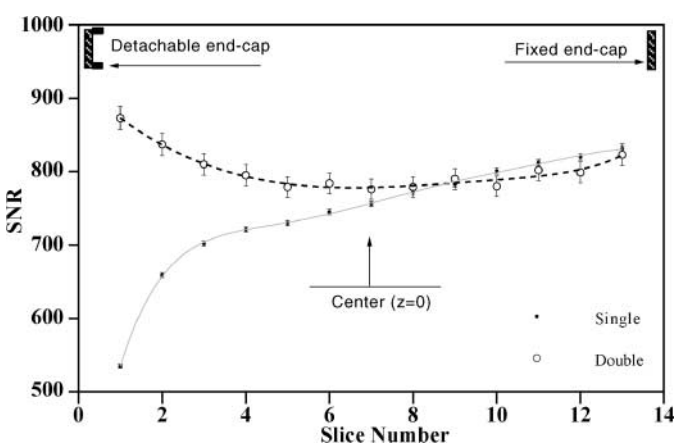

FIG. 2. The signal-to-noise ratio along the z-axis for the single end-cap and the double end-cap coils.

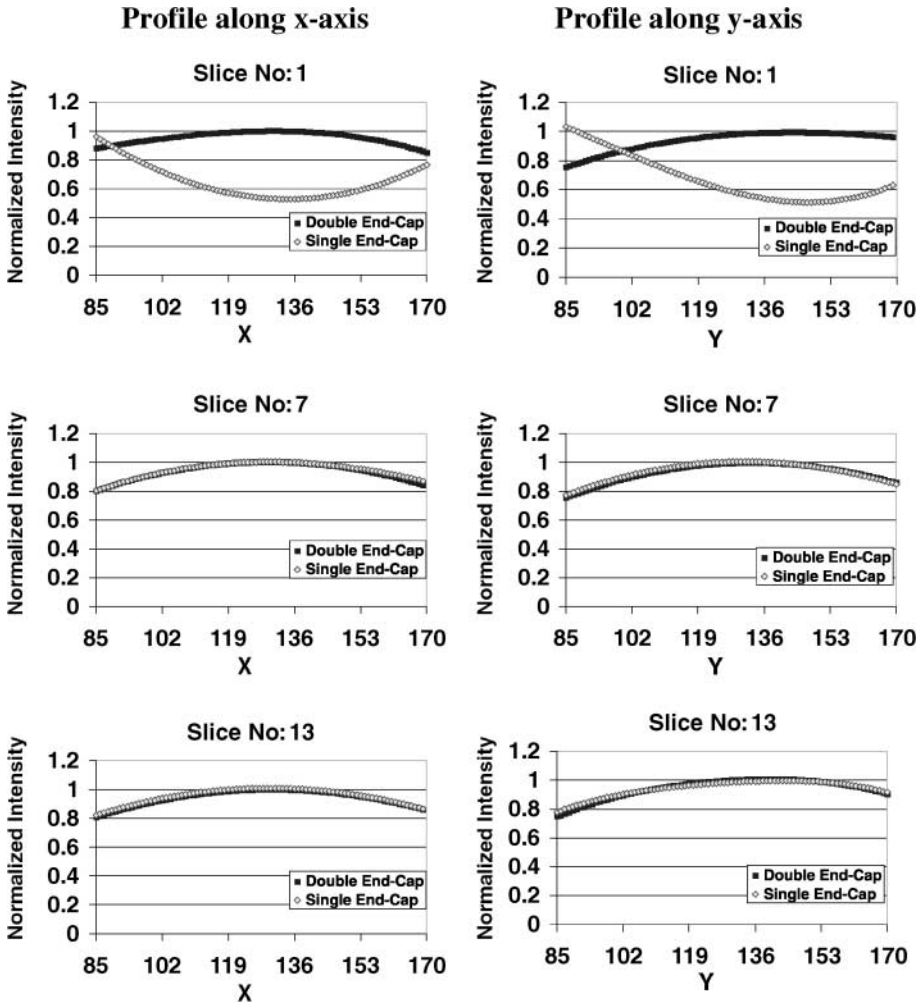

FIG. 3. The normalized intensity profile along the x- and y-axes for both double end-cap and single end-cap coils (slices 1, 7, and 13).

coils. However, the maximum change in the x- and y-profiles between slices 7 and 2 was nearly 50% for the single end-cap coil, while it was kept around 10% for the double end-cap coil. This shows that the axial response of the double end-cap coil is equal or better depending on the slice location, while there is a significant improvement along the z-direction as seen in Fig. 2.

DISCUSSION

We have shown that the double end-cap RF coil has an excellent response profile along the z-axis from one end to the other. As seen in Fig. 3, the double end-cap preserved the signal profile along x- and y-axes throughout the whole volume. Even though the profile along the y-axis was disturbed near the detachable end, maximum 10%, it was still much better than the signal profile of the single end-cap near the open end. In addition, Fig. 3 shows that the azimuthal symmetry was maintained at an adequate level. Although holders were used to center the phantom in the coil, any offset from the center of the coil as well as the movement of the phantom or coil during the removal and replacement of the end-cap may also have contributed to the error in the profiles. In the present design one end-cap is fixed while the other end-cap is detachable. The 1.6-mm gold-plated connectors provide rigid connections. The detachable end-cap of the double end-cap coil permits its use in small animal imaging. The length of the double end-cap coil could also be shorter than the single end-cap coil to get the same homogeneity throughout a certain volume; therefore it could have a higher filling factor that leads to an increase in the signal-to-noise ratio. The double end-cap coil provides a homogeneous response along its entire axis, thus enabling high quality small animal whole body imaging studies, especially when whole body imaging is required such as in dynamic contrast enhanced MRI. Furthermore, the superior homogeneity it provides can be helpful in studies involving metastatic tumor models. In these models, multiple distant tumors requiring whole body imaging can occur and the double end-cap coil described here can make such imaging possible.

ACKNOWLEDGMENTS

This research was supported in part by PHS Grant P20 CA86182 awarded by the National Cancer Institude.

REFERENCES

1. C. E. Hayes, W. A. Edelstein, J. F. Schenck, O. M. Mueller, and M. Eash, An efficient, highly homogeneous radiofrequency coil for whole-body NMR imaging at 1.5 T, *J. Magn. Reson.* **63,** 622–628 (1985).
2. C. E. Hayes, An endcap birdcage resonator for quadrature head imaging, Abstracts of the society of Magnetic Resonance in Medicine, 5th Annual Meeting, pp. 39–40, 1986.
3. A. Leroy-Wilig, L. Darrase, J. Taquin, and M. Sauzad, The slotted cylinder: an efficient probe for NMR imaging, *Magn. Reson. Med.* **2,** 20 (1985).
4. Z. Wang, M.-Y. Su, and O. Nalcioglu, Applications of dynamic contrast enhanced MRI in oncology: Measurement of tumor oxygen tension, *Techn. Cancer Res. Treatment* **1,** 1 (2002).
5. E. C. Wong, E. Boskoamp, and J. S. Hyde, A volume optimized quadrature elliptical end-cap birdcage brain coil, Abstracts of the Society of Magnetic Resonance in Medicine, 11th Annual Meeting, Vol. 2, p. 4105, 1992.